# Zeeman Effect Induced by Intense Laser Light

E. Stambulchik and Y. Maron
*Faculty of Physics, Weizmann Institute of Science, Rehovot 7610001, Israel*
(Received 14 May 2014; published 19 August 2014; corrected 20 August 2014)

We analyze spectral line shapes of hydrogenlike species subjected to fields of electromagnetic waves. It is shown that the magnetic component of an electromagnetic wave may significantly influence the spectra. In particular, the Zeeman effect induced by a visible or infrared light can be experimentally observed using present-day powerful lasers. In addition, the effect may be used for diagnostics of focused beam intensities achieved at existing and newly built laser facilities.

DOI: 10.1103/PhysRevLett.113.083002 PACS numbers: 32.60.+i, 32.70.-n, 52.70.La

Effects of oscillating electric fields on atomic spectra have been studied since the work of Blokhintsev [1] at the dawn of modern quantum mechanics. It follows from Ref. [1] that a single-Stark-component model hydrogen line in an $\vec{F}_0 \cos \Omega t$ field is split into an infinite number of satellites separated from the line center by $\pm k\Omega$, where $k$ is an integer. If, on the other hand, the field is circularly polarized, each static Stark-shifted component is split into two satellites, separated approximately by $\pm\Omega$, as found by Ishimura [2]. For nondegenerate atomic systems with the quadratic Stark effect, the influence of oscillating electric fields was first considered by Baranger and Mozer [3], who showed, in the weak-field limit, that a dipole-forbidden transition is split in the presence of such a field into two $\pm\Omega$-separated satellites. This work was extended by Hicks *et al.* [4] to arbitrarily strong electric fields. These effects have been employed in numerous studies, with the oscillating electric fields being due to plasma waves or powerful microwave or laser radiation; for details and an extensive bibliography up to the mid-1990s, see monographs [5–7].

Optical lasers generate electromagnetic (EM) waves in the visible or near-IR bands, i.e., $\hbar\Omega \sim 1$ eV. Evidently, observing satellites separated by a few eV is practical only for radiative transitions with energies in the range of hundreds of eV to a few keV, i.e., x rays (e.g., Refs. [8,9]); otherwise, the satellites may become intermixed with other spectral lines present in the same spectral region. Spontaneous x-ray radiation is characteristic of inner-shell transitions in species with atomic number $Z \gtrsim 10$, since the electron binding energies grow as $\sim Z^2$. However, the coupling of the atom to the electric field is $-\vec{d} \cdot \vec{F}$, where $\vec{d}$ is the dipole-moment operator, and its matrix elements *decrease* as $\sim Z^{-1}$.

Contrary to the electric field, the coupling to the magnetic field $-\vec{\mu} \cdot \vec{B}$ does *not* depend on $Z$ (here, $\vec{\mu}$ is the magnetic dipole moment of the atom). Therefore, the importance of the magnetic component of the EM field, relative to that of the electric component, should grow linearly with $Z$. Indeed, a simple estimation of the ratio between the magnetic and electric couplings of a charge, moving with velocity $v$, to an EM wave in vacuum is $v/c$, where $c$ is the speed of light. With a typical electron velocity $\alpha Z c/n$ in the Coulomb field of charge $Z$, this gives $\alpha Z/n$, where $\alpha \approx 1/137$ is the fine-structure constant and $n$ is the principal quantum number. However, to the best of our knowledge, all studies have so far neglected the magnetic field, considering only the electric component.

For concreteness, let us consider the Lyman-$\alpha$ transition ($n = 2$ to $n = 1$) in a hydrogenlike atom or ion. At first, we assume static $\vec{F}$ and $\vec{B}$ crossed at an arbitrary angle $\theta$. Without loss of generality, we choose the quantization axis $z$ along $\vec{F}$, while $\vec{B}$ lies in the $x$-$z$ plane. We further assume a purely linear Stark effect, neglecting the spin degree of freedom and interactions between levels with different $n$. With these assumptions, the ground $1s$ state remains unperturbed ($\Delta E_1 = 0$), while the $n = 2$ manifold of the total perturbation $V = -\vec{d} \cdot \vec{F} - \vec{\mu} \cdot \vec{B}$ reads as

$$V_2 = \begin{pmatrix} 0 & 0 & \frac{3}{Z}F & 0 \\ 0 & -\frac{\alpha\cos\theta}{2}B & \frac{\alpha\sin\theta}{2\sqrt{2}}B & 0 \\ \frac{3}{Z}F & \frac{\alpha\sin\theta}{2\sqrt{2}}B & 0 & \frac{\alpha\sin\theta}{2\sqrt{2}}B \\ 0 & 0 & \frac{\alpha\sin\theta}{2\sqrt{2}}B & \frac{\alpha\cos\theta}{2}B \end{pmatrix} \quad (1)$$

[from now on, we use the atomic units where $m_e = e = \hbar = 1/(4\pi\epsilon_0) = 1$; in these units, the speed of light $c$ is $1/\alpha$, while the Bohr magneton $\mu_0 = \alpha/2$]. We used the $(n, \ell, m)$ representation; i.e., the four $n = 2$ basis vectors are $|2s0\rangle$, $|2p-1\rangle$, $|2p0\rangle$, and $|2p+1\rangle$.

With only $F$ or $B$ present, the eigenvalue solutions of $\det(V_2 - \Delta E_2) = 0$ are 0 (doubly degenerate) and $\pm 3F/Z$ or $\pm\alpha B/2$, respectively. With $\vec{F}$ parallel to $\vec{B}$, $\vec{d} \cdot \vec{F}$ and $\vec{\mu} \cdot \vec{B}$ commute; therefore, the eigenvalues are $\pm 3F/Z$ and $\pm\alpha B/2$, i.e., a combination of the lateral Stark and Zeeman patterns. The relative effect of the magnetic field is, thus,

 

$$\xi \equiv \frac{\alpha Z}{6}\frac{B}{F}. \tag{2}$$

However, if $\vec{F}$ and $\vec{B}$ are perpendicular, the solution is different: There again appears the doubly degenerate unshifted component, while the two lateral components are shifted by $\pm\sqrt{(3F/Z)^2+(\alpha B/2)^2}$, i.e.,

$$\Delta E_2 = \left\{0, \pm\frac{3F}{Z}\sqrt{1+\xi^2}\right\}. \tag{3}$$

Therefore, the Stark-Zeeman pattern becomes that of the pure Stark effect in an "effective" field $F' = F\sqrt{1+\xi^2}$. In an EM wave propagating in vacuum or in a media with the refraction index close to unity (such as an underdense plasma), $\vec{F}$ and $\vec{B}$ are perpendicular and equal by absolute value, i.e., $\xi = \alpha Z/6$. Therefore, even for transuranium elements, the correction due to the magnetic field is only about 1%.

Thus, at first sight, the neglect of the magnetic component appears to be justified. However, so far, we have omitted the spin degree of freedom. Including it makes a crucial difference. The fine structure due to the spin-orbit interaction $V_{\ell s} = A_{n\ell}\vec{L}\cdot\vec{S}$ results in splitting of an $n\ell$ ($l > 0$) level into $j = \ell + \frac{1}{2}$ and $j = \ell - \frac{1}{2}$ levels shifted by $A_{n\ell}\ell/2$ and $-A_{n\ell}(\ell+1)/2$, respectively, where

$$A_{n\ell} = \frac{\alpha^2 Z^4}{n^3\ell(\ell+1)(2\ell+1)} \tag{4}$$

(e.g., see Ref. [10]; the Lamb shift is neglected). In the ($n$, $\ell$, $m$, $m_s$) representation, the $n = 2$ subset of the perturbation is then

$$V_2 = \begin{pmatrix} -a & b & 0 & 0 & f & 0 & 0 & 0 \\ & -a & 0 & 0 & 0 & f & 0 & 0 \\ & & \frac{a}{2} & b & \frac{b}{\sqrt{2}} & 0 & 0 & 0 \\ & & & -\frac{a}{2} & \frac{a}{\sqrt{2}} & \frac{b}{\sqrt{2}} & 0 & 0 \\ & & & & 0 & b & \frac{b}{\sqrt{2}} & 0 \\ & & & & & 0 & \frac{a}{\sqrt{2}} & \frac{b}{\sqrt{2}} \\ & & & & & & -\frac{a}{2} & b \\ & & & & & & & \frac{a}{2} \end{pmatrix}, \tag{5}$$

where $f \equiv 3F/Z$, $b \equiv \alpha B/2$, and $a \equiv A_{2p}$ (the lower triangle of the symmetric matrix is not shown). Assuming smallness of $b$ (i.e., omitting terms containing the second and higher orders of $b$ in the characteristic polynomial), one obtains doubly degenerate $\Delta E_2 = a/2$ and six roots of cubic equations

$$2\Delta E_2{}^3 + \Delta E_2{}^2(3a+4b) - 2\Delta E_2(f^2 - 3ab) = a(f^2 - 2ab + a^2) \tag{6}$$

and a similar one with $b \to -b$. The explicit expressions are straightforward but cumbersome.

Evidently, if $f, b \gg a$, the Stark-Zeeman pattern reduces to that of Eq. (3). The opposite, weak-field limit ($f, b \ll a$) is obviously not interesting. Let us instead consider the case of $b \lesssim a \ll f$. In this case,

$$\Delta E_2 \approx \left\{\pm\frac{a}{2}, \pm\sqrt{f^2+b^2} \pm b - \frac{a}{2}\right\}. \tag{7}$$

The $n = 1$ perturbation Hamiltonian is

$$V_1 = \begin{pmatrix} 0 & b \\ b & 0 \end{pmatrix}, \tag{8}$$

giving

$$\Delta E_1 = \pm b. \tag{9}$$

Importantly, the upper-state energies depend, in general, on $f$ and $b$, while those of the lower states depend only on $b$. The $\pm b$ contribution to the energies of the upper lateral and lower states correspond to different spin orientations along the magnetic field; since spin-flipping transitions are dipole forbidden, the lateral components of the Lyman-$\alpha$ transition appear at

$$\Delta E^{(\text{lateral})} \approx \pm\sqrt{f^2+b^2} - \frac{a}{2} = \pm\frac{3F}{Z}\sqrt{1+\xi^2} - \frac{A_{2p}}{2}, \tag{10}$$

i.e., up to a constant shift, the same as in the no-spin approximation (3), with a negligible magnetic-field effect. However, the central component that remains unshifted in the no-spin approximation becomes split into four components

$$\Delta E^{(\text{central})} \approx \pm\frac{a}{2} \pm b = \pm\frac{1}{2}(A_{2p} \pm \alpha B), \tag{11}$$

the positions of which depend *linearly* on $B$.

Although derived assuming $f \gg a$, these results also remain qualitatively valid if $f \simeq a$. As an example, the combined Stark-Zeeman effect of the Lyman-$\alpha$ transition in Kr XXXVI (hydrogenlike Kr ion) under the static $F$ and $B$ fields, approximately corresponding to those in the laser light focused to an intensity of $10^{20}$ W/cm$^2$, is shown in Fig. 1. For the numerical calculations, the atomic energies were taken from the NIST database [11], thus also accounting for the Lamb shift; the effect of the latter was, as expected, mostly negligible for the

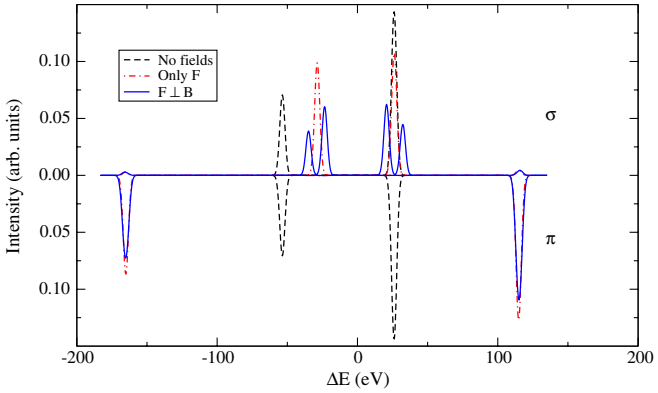


FIG. 1 (color online). Combined static Stark-Zeeman effect of Kr XXXVI Ly-$\alpha$ in the perpendicular electric and magnetic fields. The $\sigma$ and $\pi$ polarization components are given separately. For comparison, zero-field and electric-field-only spectra are also shown. $F_z = 30$ TV/m and $B_x = 100$ kT are assumed. Zero on the energy axis corresponds to the Kr XXXVI Ly-$\alpha$ unperturbed energy of ≈13.5 keV [11].

field strengths assumed. Contrary to the calculations with the fine-structure effect omitted, the magnetic field causes a significant, $\approx \alpha B$, splitting of the central components.

An important characteristic of the spectrum is its polarization properties, unsurprisingly very similar to those of the pure Stark effect: The central and lateral components are mostly $\sigma$ and $\pi$ polarized, respectively. Therefore, with a proper direction of observation (parallel to $\vec{F}$) or using a polarizer, the $\pi$ components can be suppressed, thus simplifying observation of the Zeeman effect in the central part of the spectrum.

Let us now consider the time-dependent effect in the presence of a harmonic EM field. To this end, we employ a computer simulation technique [12], modified to use, instead of the plasma microfields, macroscopic fields as a perturbation:

$$\vec{F}(t) = \vec{F}_0 \sin(\Omega t),$$
$$\vec{B}(t) = \vec{B}_0 \sin(\Omega t), \tag{12}$$

where $\vec{F}_0$ and $\vec{B}_0$ are orthogonal and equal in absolute value; that is, they are components of a linearly polarized EM wave. The results are shown in Fig. 2(a). Although the spectrum is composed of an infinite number of satellites, separated by $\hbar\Omega$ (the inset shows a small portion of the graph zoomed in), it retains the important features inferred from the static solution (Fig. 1): (i) the central components are split by the magnetic field, and (ii) the Zeeman effect can be isolated and enhanced by choosing an appropriate direction of observation or polarization. These features become especially apparent after convolution of the spectrum with a smoothing function, as shown in Fig. 2(b).

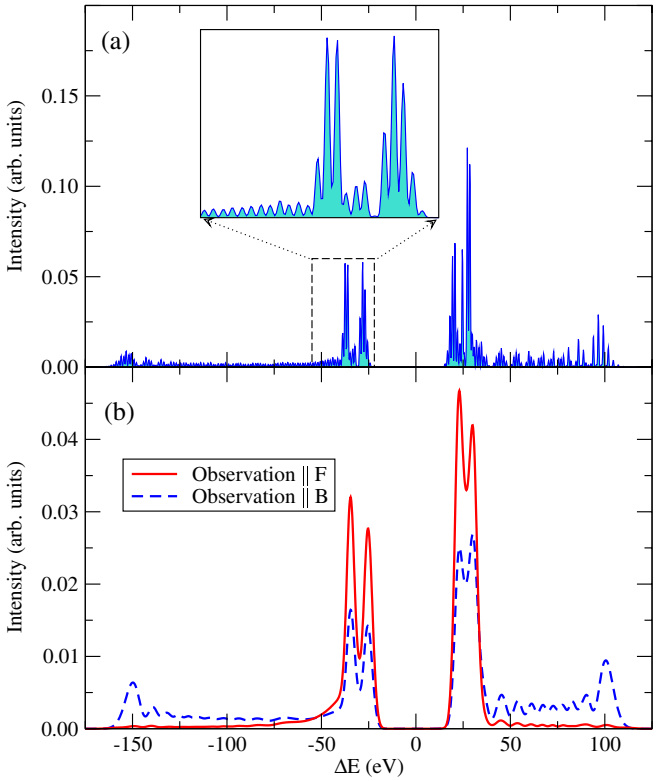


FIG. 2 (color online). (a) Combined Stark-Zeeman effect of Kr XXXVI Ly-$\alpha$ in the EM field of a linearly polarized light with intensity $10^{20}$ W/cm$^2$ and angular frequency $\Omega = 2 \times 10^{15}$ rad/s ($\lambda \approx 0.94$ $\mu$m), averaged over all directions of observation. (b) Same after convolution with a 4-eV FWHM Gaussian and shown separately for directions of observation parallel to $\vec{F}$ or $\vec{B}$ of the laser field.

Evidently, higher intensities and, hence, stronger magnetic fields would result in a more pronounced Zeeman effect. For such strong fields, however, the linear-Stark-effect approximation is no longer justified, and higher-order Stark effects (arising mostly due to electric-field-induced mixing between the $n = 2$ and $n = 3$ states) need to be accounted for, resulting in "redshifts" of the Ly-$\alpha$ components. Such calculations are shown in Fig. 3. One sees that by varying the laser intensity, the spectral pattern changes significantly.

The effect is important and can be observed in many species, provided a few criteria are satisfied. The first one, already discussed, is that $b \lesssim a \lesssim f$. With the laser mean-squared field magnitudes $\langle F \rangle = \langle B \rangle = \sqrt{4\pi\alpha I}$, where $I$ is the laser beam intensity, this condition can be rewritten as

$$\frac{\alpha^{3/2} Z^5}{288} \lesssim \sqrt{\pi I} \lesssim \frac{\alpha^{1/2} Z^4}{48}. \tag{13}$$

The natural linewidth $\Gamma$, determined by the spontaneous radiative rate, should be smaller than the Zeeman splitting, i.e., $\Gamma \lesssim b$, or [10]

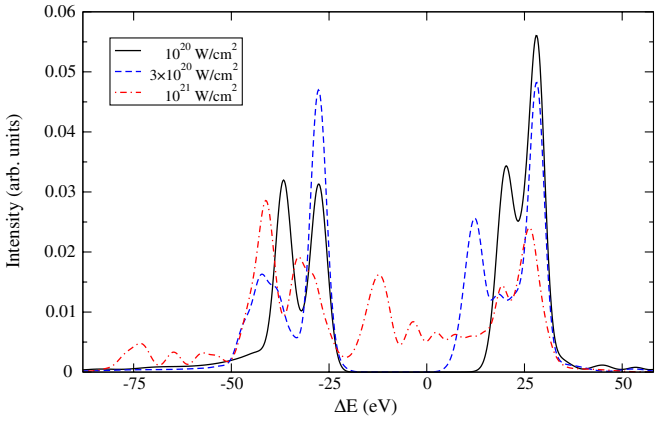


FIG. 3 (color online). Combined Stark-Zeeman effect of Kr XXXVI Ly-$\alpha$ in the EM field of a linearly polarized light of varying intensity. The direction of observation is parallel to the polarization vector. The spectra are convolved with a 4-eV FWHM Gaussian.

$$\sqrt{\pi I} \gtrsim \frac{64\alpha^{3/2}Z^4}{2187}. \tag{14}$$

In addition, the laser intensity should not be too high to cause field ionization of the upper ($n = 2$) level. Using the classical ionization field (e.g., Ref. [13]) as an estimate, this criterion gives

$$\sqrt{\pi I} \lesssim \frac{Z^3}{512\alpha^{1/2}}. \tag{15}$$

Inequalities (13)–(15) are represented graphically in Fig. 4; the area in the $(Z, I)$ plane for which all these four conditions are simultaneously satisfied is filled with a light gray color. Two additional criteria are less general. Similarly to the $f/\Omega \gtrsim 1$ [5,6] requirement for the Stark effect to be pronounced, in the case of the Zeeman effect, for the same reason, $b/\Omega \gtrsim 1$ should be satisfied, i.e.,

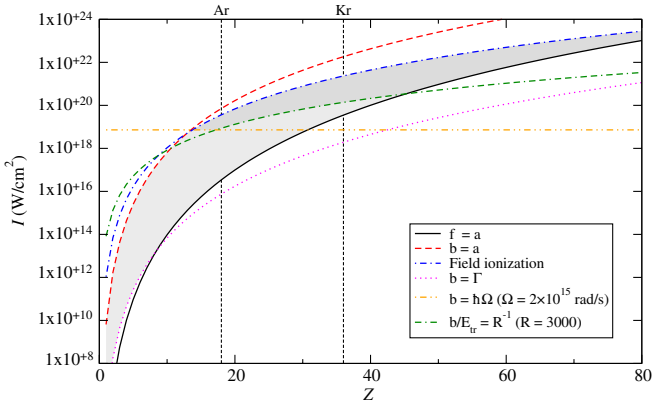


FIG. 4 (color online). Criteria and regions of observability of the Zeeman effect on Ly-$\alpha$ of species with the atomic number $Z$ in the EM field with intensity $I$ (see the text).

$$\sqrt{\pi I} \gtrsim \frac{\Omega}{\alpha^{3/2}}. \tag{16}$$

Finally, for observing the effect, it must be resolved, i.e., $b \gtrsim \Delta E$, where $\Delta E$ is the contribution to the linewidth due to both the Doppler and instrumental broadenings. Thus,

$$\sqrt{\pi I} \gtrsim \frac{3Z^2}{8\alpha^{3/2}R}, \tag{17}$$

where $R = E_{\rm tr}/\Delta E$, and $E_{\rm tr} \approx 3Z^2/8$ is the Ly-$\alpha$ transition energy. With $\Omega = 2 \times 10^{15}$ rad/s and $R = 3000$ (see below), these additional criteria result in a further narrowing down of the region of observability, shown by the darker gray area in Fig. 4. One can see, for example, that the effect is important for the Ar Ly-$\alpha$ transition in the laser-intensity range of approximately $(1\text{–}4) \times 10^{19}$ W/cm$^2$, whereas for Kr Ly-$\alpha$, the relevant range is $(1\text{–}20) \times 10^{20}$ W/cm$^2$.

For a direct observation of the effect, high temporal and spatial resolutions are required, since achieving irradiation intensities $\sim 10^{20}$ W/cm$^2$ implies the use of subpicosecond laser pulses focused to a few-micrometer-diameter spot. Evidently, acquiring radiation from a larger volume or during a longer time would result in mixing of the laser-affected spectrum with the unperturbed line, making the discrimination of the interesting effect challenging. We performed calculations assuming a measurement where only one-tenth of the recorded signal is useful, for example, a laser pulse with a Gaussian envelope of 100-fs FWHM and a 1-ps time resolution of the data acquisition system; alternatively, these calculations would correspond, e.g., to a 4 times better time resolution [14] but an inferior spatial resolution, exceeding the laser-focal-spot diameter twofold. The results are shown in Fig. 5. Even with these unfavorable assumptions, the

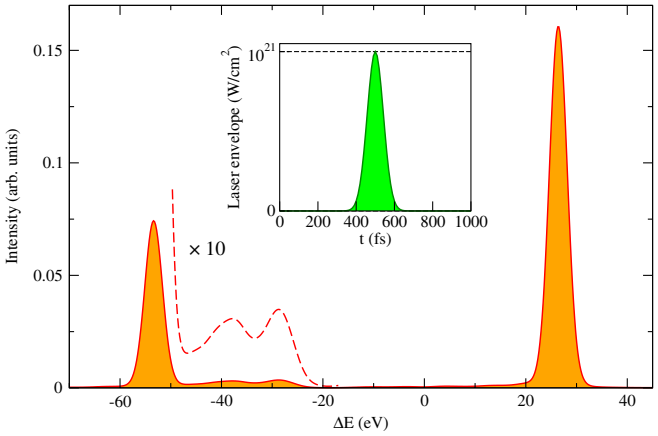


FIG. 5 (color online). Modeling of the Kr XXXVI Ly-$\alpha$ spectrum collected over a 1-ps exposure and subjected to an EM field of a linearly polarized laser with a 100-fs Gaussian envelope (shown in the inset). The direction of observation is parallel to the polarization vector. For clarity, a ×10 enlarged spectrum is shown by the dashed line.

Zeeman splitting is clearly seen at the "blue" side of the unperturbed Ly-$\alpha_{1/2}$ $(1s_{1/2} - 2p_{1/2})$ component. The plasma electrons should have a sufficiently high temperature ($kT_e \sim 3$–$6$ keV) in order to cause a significant population of the H-like $n = 2$ states. We note that the Doppler broadening is likely to be negligible, since the thermal electron-ion relaxation time for an underdense ($n_e \lesssim 10^{21}$ cm$^{-3}$) Kr plasma is on the order of 10 ns (e.g., Ref. [13]), much longer than the laser-pulse duration. Thus, the $\Delta E = 4$ eV broadening assumed in this and previous figures should be viewed largely as an instrumental broadening, corresponding to a resolving power $R = E/\Delta E \approx 3400$. Finally, the effect of the plasma microfields for the conditions assumed is completely negligible [13].

To conclude, contrary to naive expectations, the magnetic component of an EM wave may significantly influence spectra of radiative transitions. Amazingly, the Zeeman effect induced by a visible or infrared light can be experimentally observed using present-day powerful lasers. Additionally, the effect may, in principle, serve for diagnostics of focused beam intensities achieved at existing and newly built laser facilities.

We thank E. Kroupp, G. G. Paulus, O. Renner, and I. Uschmann for fruitful discussions. Valuable comments of the referees are highly appreciated. This work was supported in part by the Minerva Foundation (Germany) and the Cornell Center of Excellence for the Study of Pulsed-Power-Driven High Energy Density Plasma Studies.

[1] D. I. Blochinzew, Phys. Z. Sowjetunion **4**, 501 (1933).
[2] T. Ishimura, J. Phys. Soc. Jpn. **23**, 422 (1967).
[3] M. Baranger and B. Mozer, Phys. Rev. **123**, 25 (1961).
[4] W. W. Hicks, R. A. Hess, and W. S. Cooper, Phys. Rev. A **5**, 490 (1972).
[5] V. S. Lisitsa, *Atoms in Plasmas*, Springer Series on Atoms and Plasmas Vol. 14 (Springer, Berlin, 1994).
[6] E. Oks, *Plasma Spectroscopy: The Influence of Microwave and Laser Fields*, Springer Series on Atoms and Plasmas Vol. 9 (Springer, Berlin, 1995).
[7] H. R. Griem, *Principles of Plasma Spectroscopy* (Cambridge University Press, Cambridge, England, 1997).
[8] O. Renner, O. Peyrusse, P. Sondhauss, and E. Förster, J. Phys. B **33**, L151 (2000).
[9] N. C. Woolsey, D. M. Chambers, C. Courtois, E. Förster, C. D. Gregory, I. M. Hall, J. Howe, O. Renner, and I. Uschmann, J. Quant. Spectrosc. Radiat. Transfer **99**, 680 (2006).
[10] H. A. Bethe and E. E. Salpeter, *Quantum Mechanics of One- and Two-Electron Atoms* (Plenum, New York, 1977).
[11] A. Kramida, Yu. Ralchenko, J. Reader, and the NIST ASD Team, NIST Atomic Spectra Database (version 5.1), http://physics.nist.gov/asd.
[12] E. Stambulchik and Y. Maron, J. Quant. Spectrosc. Radiat. Transfer **99**, 730 (2006).
[13] E. Stambulchik and Y. Maron, JINST **6**, P10009 (2011).
[14] J. Feng, H. J. Shin, J. R. Nasiatka, W. Wan, A. T. Young, G. Huang, A. Comin, J. Byrd, and H. A. Padmore, Appl. Phys. Lett. **91**, 134102 (2007).